Electronic Supplementary Material (ESI) for Physical Chemistry Chemical Physics.
This journal is © the Owner Societies 2019

Electronic Supplementary Information for:

MARTINI-based Simulation Method for Step-growth Polymerization and its Analysis by Size Exclusion Characterization: A Case Study of Cross-linked Polyurethane

Hassan Ghermezcheshme[†], Hesam Makki [†*], Mohsen Mohseni [†*], Morteza Ebrahimi[†], Gijsbertus de With[‡]

[†] Amirkabir University of Technology, Department of Polymer and Color Engineering, 424 Hafez Ave., Tehran, Iran

[‡] Eindhoven University of Technology, Laboratory of Physical Chemistry, Department of Chemical Engineering & Chemistry, POB 513, NL-5600 MB Eindhoven, The Netherlands

*** Corresponding authors:**

Hesam Makki, Phone: +9821 6454 2434, E-mail: hmakki@aut.ac.ir

Mohsen Mohseni, Phone: +9821 6454 2441, E-mail: mmohseni@aut.ac.ir

1 - Atomistic Parameters

MD simulations were adjusted employing the COMPASS (condensed-phase optimized molecular potentials for atomistic simulation studies) force field[1] to perform simulations for a simulation box containing 100 cross-linker molecules. After geometry optimization, MD simulations were performed using *NVT* (T = 25 °C) conditions with 1 fs time step for 100 ps. This simulation step was done by coupling the system to Berendsen thermostat. Thereafter, the simulation continued at *NPT* conditions (P = 1 bar, T = 25 °C) with a 1 fs time step and 500 ps duration. A Nosé-Hoover thermostat and Parrinello-Rahman barostat were selected for controlling the temperature and pressure for this step, respectively. The average distributions of bonds and angles for selected atoms were plotted. The probability converted to potential by means of equation ESI-1:

$$U = -\ln(p)kT \qquad \text{(ESI-1)}$$

where U is the potential, p the probability, k Boltzmann constant and T temperature. The equilibration values and force constants for bond lengths and angles were obtained by fitting equations 2 and 3 to the potential-distance and potential-angle distributions, respectively.

$$U_{bond} = K_{bond}(l - l_0)^2 \qquad \text{(ESI-2)}$$

$$U_{angle} = K_{angle}(\theta - \theta_0)^2 \qquad \text{(ESI-3)}$$

The values obtained for K_{bond}, K_{angle}, l_0 and θ_0 for the selected atoms are listed in Table ESI-1 and ESI-2. For dihedral angle interactions, the corresponding sequence of atoms in the OPLS-AA force field was used. Ryckaert-Bellemans dihedral types are used and the constants are listed in Table ESI-3.

The structure of cross-linker is shown in Fig. ESI-1.

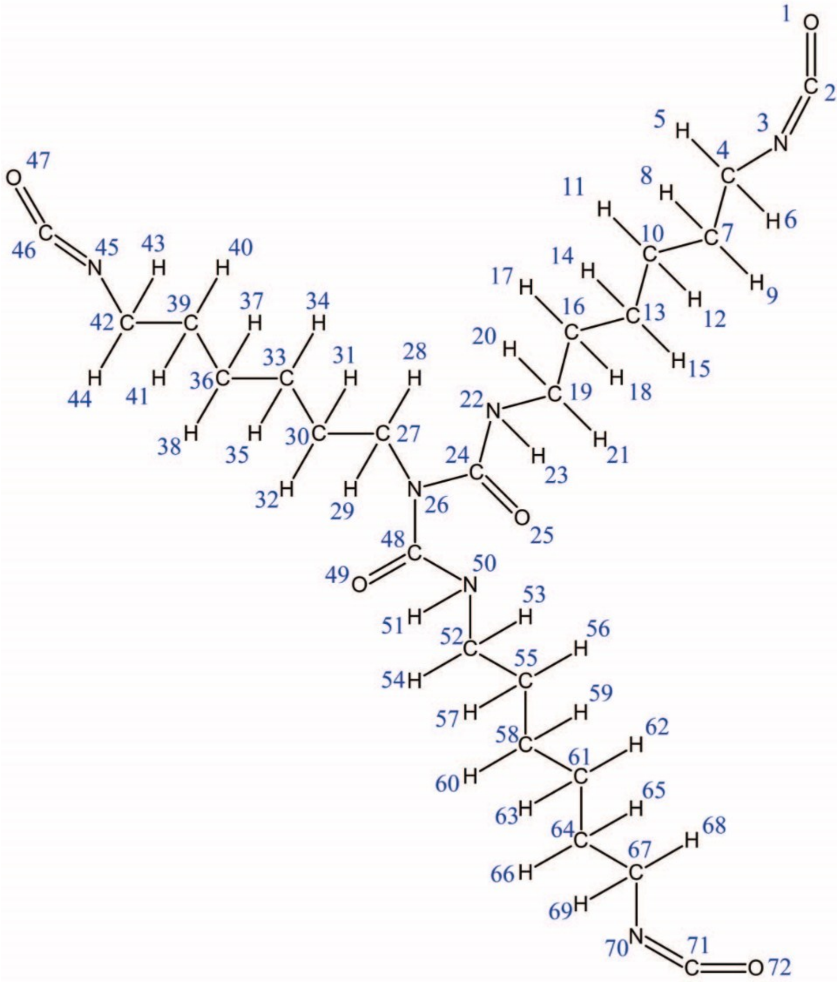

Fig. ESI-1 The structure of cross-linker. A number is assigned to each atom to define bond and angle parameters.

Table ESI-1 Bond type parameters at atomistic level for cross-linker.

Bond	**l_0 (nm)**	**K_{bond} (kJ/mol nm^2)**
1-2	0.116	432600
2-3	0.120	360800
3-4	0.148	120800
4-5,4-6	0.120	382300
19-20, 19-21	0.111	133900
19-22	0.148	106800
22-23	0.102	174000
22-24	0.138	163400
24-25	0.122	308300
24-26	0.140	168400
26-27	0.148	122600
27-28, 27-29	0.111	130000

Table ESI-2 Angle type parameters at atomistic level for cross-linker.

Angle	θ_0 (º)	K_{angle} (kJ/mol rad^2)
1-2-3	169.6	228.6
2-3-4	142.3	202.8
3-4-5, 4-5-6	106.9	295.4
3-4-7	116.1	252.2
16-19-22	114.7	238.6
20-19-22, 21-19-22	108.3	281.8
19-22-23	111.2	206.5
19-22-24	120.6	250.0
23-22-24	116.0	161.5
22-24-25	119.4	609.4
22-24-26	119.1	606.6
25-24-26	121.6	665.0
24-26-27	119.3	387.6
24-26-48	116.5	244.7
26-27-28, 26-27-29	108.4	281.3
26-27-30	116.0	263.5

Table ESI-3 Dihedral type parameters at atomistic level for cross-linker.

Dihedral	C_0 (kJ/mol)	C_1 (kJ/mol)	C_2 (kJ/mol)	C_3 (kJ/mol)	C_4 (kJ/mol)	C_5 (kJ/mol)
1-2-3-4	25.47638	0	-25.47638	0	0	0
2-3-4-7	21.3384	-0.8368	-20.5016	0	0	0
3-4-7-10	-0.76567	2.70705	4.02501	-5.96639	0	0
4-7-10-13	-4.23421	7.22159	1.9079	-4.89528	0	0
10-13-16-19	-4.23421	7.22159	1.9079	-4.89528	0	0
13-16-19-22	-0.76567	2.70705	4.02501	-5.96639	0	0
16-19-22-24	21.3384	-0.8368	-20.5016	0	0	0
19-22-24-25	25.47638	0	-25.47638	0	0	0
22-24-26-27	33.20422	0	-33.20422	0	0	0
24-26-27-30	21.3384	-0.8368	-20.5016	0	0	0
25-24-26-27	25.47638	0	-25.47638	0	0	0
26-27-30-33	-0.76567	2.70705	4.02501	-5.96639	0	0
27-30-33-36	-4.23421	7.22159	1.9079	-4.89528	0	0
26-24-22-19	33.20422	0	-33.20422	0	0	0

After obtaining the missing parameters for the OPLS-AA force field, the first step of MD simulations is energy minimization. 100 molecules of each material were minimized individually until the change in energy is less than 1000 kJ/mol.nm. After that, the simulation was continued at a constant temperature (227 °C) and constant volume (*NVT* step) for 500 ps with 2 fs time step using a modified Berendsen thermostat. Thereafter, simulations at *NPT* conditions (P = 1 bar, T = 227 °C) were started with a 0.5 fs time step and 5 ns duration. For this step we used a modified Berendsen thermostat and Parrinello-Rahman barostat. The finally, cooling was done from 227 °C to 27 °C with a rate of 0.04 °C /ps. After cooling, the equilibrium was obtained at *NPT* conditions (P = 1 bar, T = 27 °C), similar to the first *NPT* step.

2 - Coarse-Grained (CG) Parameters

Based on MARTINI method, the bonded interactions were described by means of equation ESI-4 and ESI-5 for the bond and angle interactions, respectively. To obtain force constants and equilibrium values for the bond and angle potentials, the following procedure was carried out. Initially, the distributions of the bonds and angles connecting the centers of mass of the atoms of a bead were averaged over 5 ns trajectories obtained from the atomistic simulation. The distribution of bonds and angles was converted to probability and the values of the potentials obtained by equation ESI-1. The force constants for bonds and angles were obtained by fitting equation ESI-4 and ESI-5 to potential-distance and potential-angle distributions, respectively. Table ESI-4 and ESI-5 contain the equilibrium values and force constants for all bonded interactions at the CG level. For simplicity, we ignored torsional potentials at the CG level.

$$U_{bond} = \frac{1}{2}K_{bond}(l - l_0)^2 \tag{ESI-4}$$

$$U_{angle} = \frac{1}{2}K_{angle}[\cos(\theta) - \cos(\theta_0))]^2 \tag{ESI-5}$$

Table ESI-4 Bond type parameters at CG level.

Bond	l_0 (nm)	K_{bond} (kJ/mol.nm^2)
Triisocyanate Cross-linker		
NCO-CC1	0.2963	15732
CC1-CC1	0.2408	32040
CC1-NCC	0.2817	12484
NCC-CONH	0.2780	13600
CONH-CC1	0.2779	16366
PTMG		
COH-CC1	0.2399	29340
CC1-COC	0.2836	11446
mPEG		
COH-COC	0.2692	7686
COC-COC	0.3119	4810
COC-COM	0.3130	5140
Urethane		
UOH-UNCO	0.4000	10000
CC1-UNCO	0.2963	15732
COC-UOH	0.2692	7686
CC1-UOH	0.2399	29340
Normal butyl acetate		
CC1-CC1	0.2620	18640
CC1-OCOM	0.2970	19810

Table ESI-5 Angle type parameters at CG level.

angle	θ_0 (°)	K_{angle} (kJ/mol.rad^2)
Triisocyanate Cross-linker		
NCO-CC1-CC1	109.73	41.62
CC1-CC1-NCC	163.94	152.56
CC1-NCC-CONH	136.12	197.84
NCC-CONH-CC1	120.73	566.60
CONH-CC1-CC1	118.91	73.22
CC1-CC1-CC1	157.00	474.80
CONH-NCC-CONH	74.00	122.00
PTMG		
COH-CC1-COC	153.00	170.00
CC1-COC-CC1	133.00	55.80
COC-CC1-COC	150.08	78.62

mPEG		
COH-COC-COC	114.24	38.10
COC-COC-COC	121.43	35.42
COC-COC-COM	119.90	38.50
Urethane		
COC-CC1-UOH	153.00	170.00
CC1-UOH-UNCO	150.00	100.00
UOH-UNCO-CC1	150.00	100.00
UNCO-CC1-CC1	109.73	41.62
COC-COC-UOH	114.24	38.10
COC-UOH-UNCO	150.00	100.00
Normal butyl acetate		
CC1-CC1-OCOM	141.05	25.86

Non-bonded interactions for beads at the CG level are described by Lennard-Jones 12-6 potential energy functions. The values of σ, the distance between two particles at energy zero, and ε, the strength of the interaction for each pair of beads are directly taken from the MARTINI force-field based on our bead typing. The validity of the bonded and non-bonded interactions is checked by comparison of the density at the atomistic and CG level, see Table 1.

3 - Glass transition temperature T_g

For calculating the T_g, the materials were heated up to 127 °C with time step of 10 fs during 50 ns. After that the system is cooled down from 127 °C to −73 °C during 500 ns with a time step of 10 fs using temperature steps of 5 °C during which volume-temperature data were obtained. The modified Berendsen thermostat and Berendsen barostat were used for these two steps. For each step, the average of volume versus temperature is plotted and T_g is taken as the intersection of the rubbery and glassy region for the volume-temperature curve. As an example, the volume-temperature curves of case II for two states, before the beginning of the reaction and after final conversion, are shown in Fig. ESI-2. The volume-temperature curves for cases IV, V and VI are shown in Fig. ESI-3.

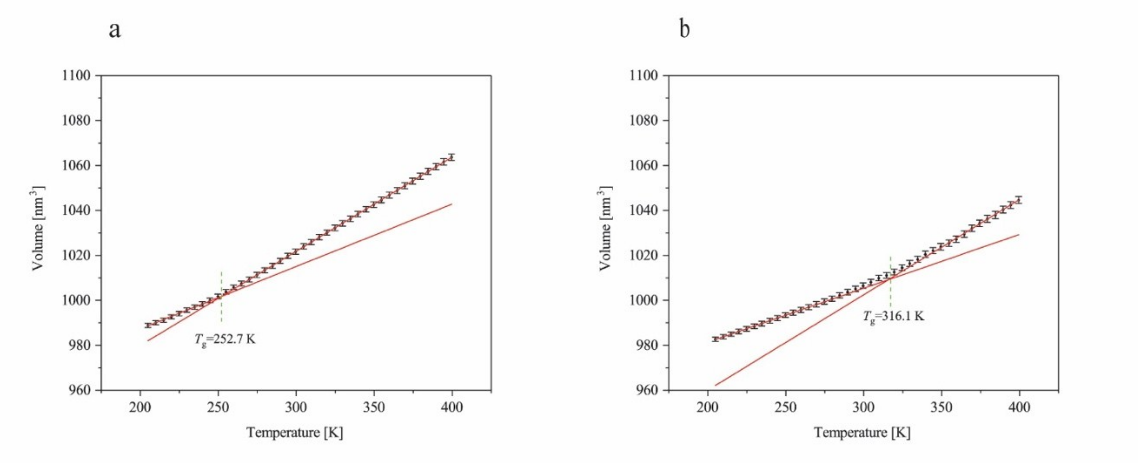

Fig. ESI-2 Volume-temperature curves for case II, a) before the beginning of cross-linking, b) after final conversion.

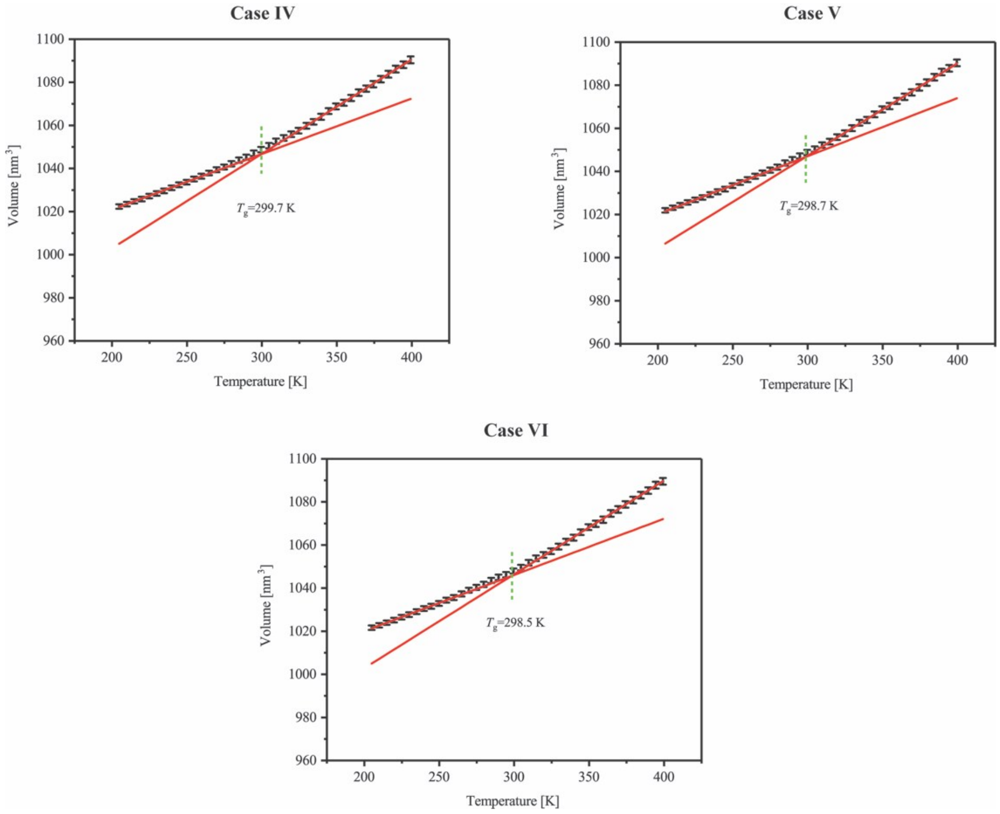

Fig. ESI-3 Volume-temperature curves for cases IV, V and VI after final conversion.

4 - Mean squared displacement

Fig. ESI-4 shows the diffusion coefficient for all beads as a function of conversion for case II. The diffusion coefficient is measured by linear fitting of the mean squared displacement (nm^2) of all beads as a function of time (ps) at 25 °C.

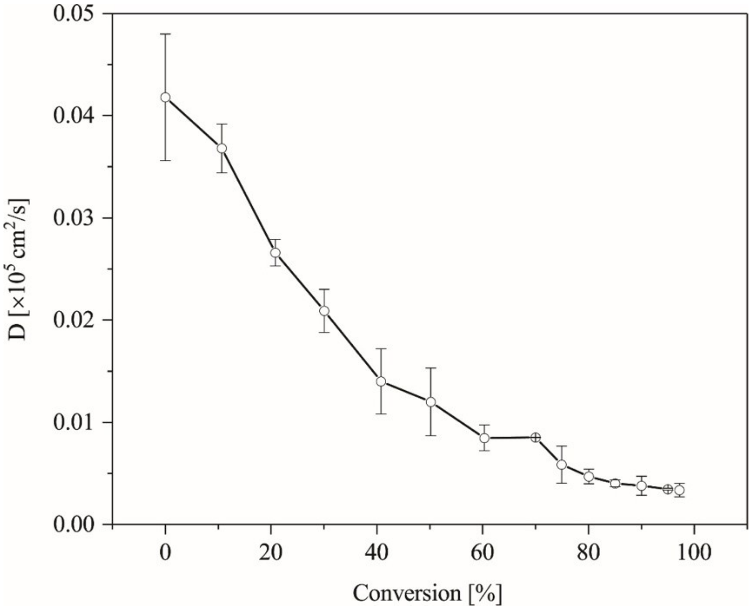

Fig. ESI-4 Diffusion coefficient *D* as a function of conversion for case II.

5 - Number average molecular weight M_n and weight average molecular weight M_w

The number average molecular weight M_n and weight average molecular weight M_w of all clusters except the largest were determined. Fig. ESI-4 shows M_n and M_w for cases II, IV, V and VI as a function of conversion.

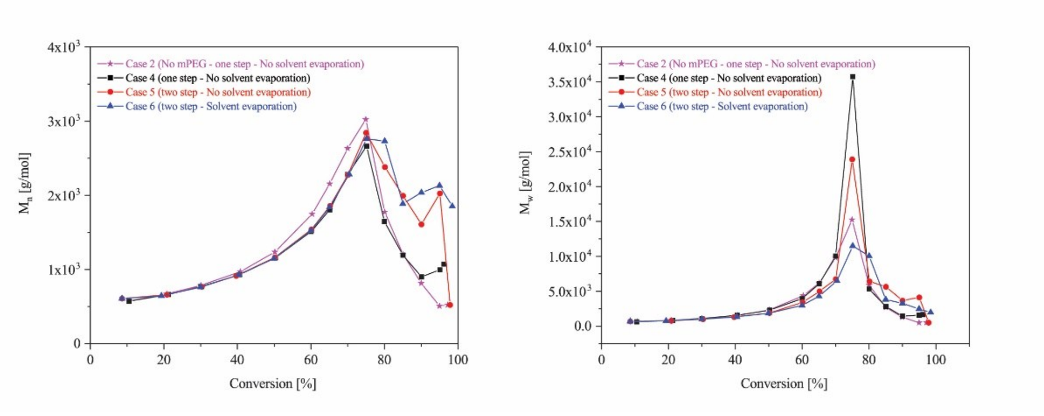

Fig. ESI-5 M_n and M_w for cases II, IV, V and VI.

6 - Phase separation

The nano-phase separation of the soft and hard segments of these PU systems was checked by visualization of the molecules as well as the density profiles of the various segments. As shown in Fig. ESI-6 and ESI-7, no significant change can be detected for the various reaction conditions.

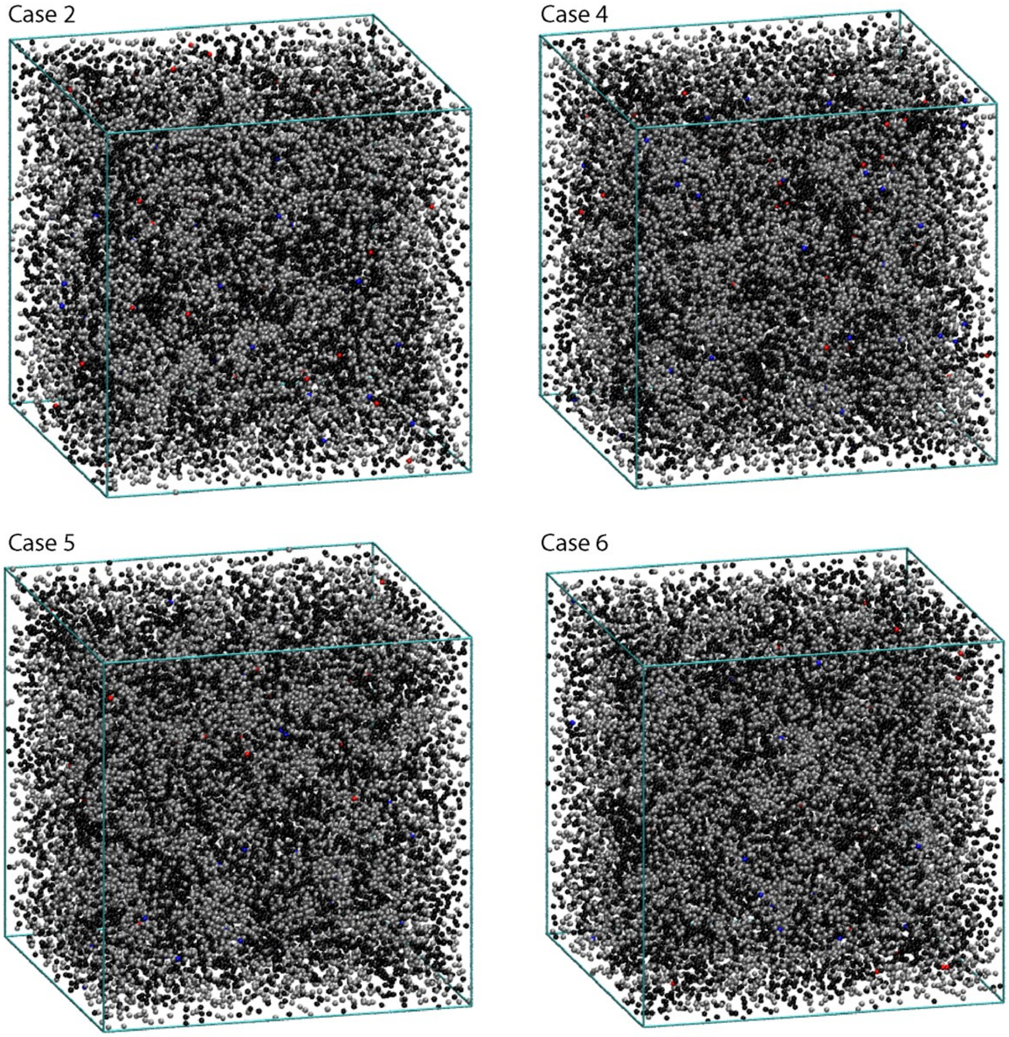

Fig. ESI-6 Soft (silver) and hard (black) segments for cases II, IV, V and VI after final conversions. The red and blue dots are unreacted NCO and OH beads.

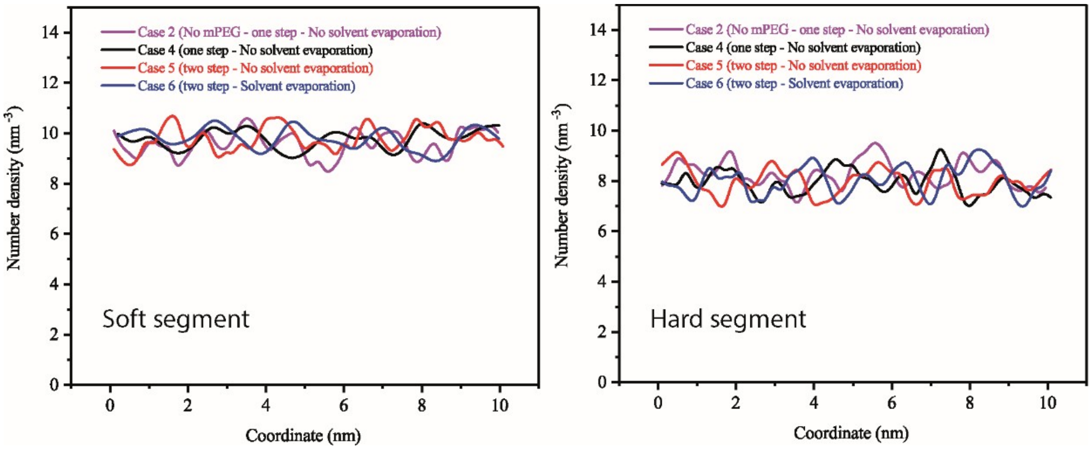

Fig. ESI-7 Density profile of soft and hard segments for cases II, IV, V and VI for 10 ns simulation.

We also studied the nano-phase separation of the mPEG dangling chains by means of visualization and density profile analysis. As shown in Fig. ESI-8 and ESI-9, only a slightly lower level of phase separation is observed for case V.

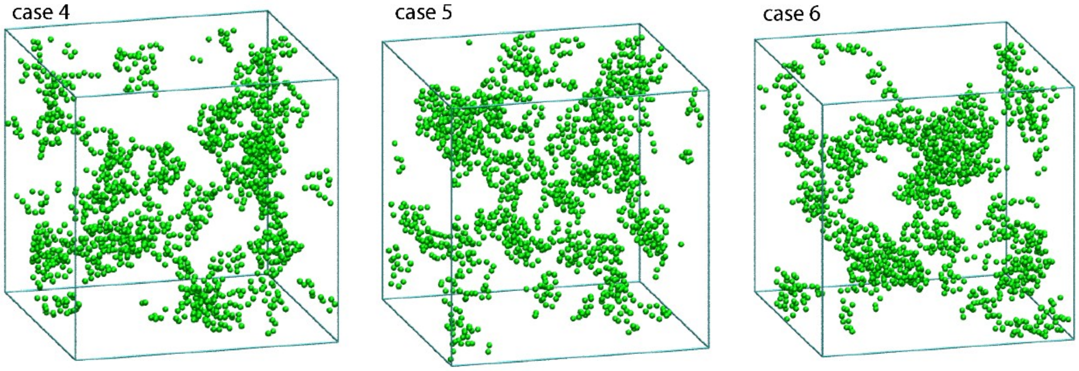

Fig. ESI-8 mPEG chains in the box for cases IV, V and VI after final conversion.

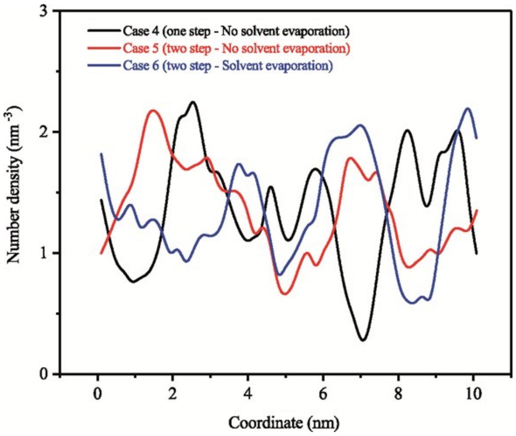

Fig. ESI-9 Density profile of mPEG chains for cases IV, V and VI for 10 ns simulation.

References

1 H. Sun, *The Journal of Physical Chemistry B*, 1998, **102**, 7338-7364.